

000 REACTID: SYNCHRONIZING REALISTIC ACTIONS AND 001 IDENTITY IN PERSONALIZED VIDEO GENERATION 002 003 004

005 **Anonymous authors**

006 Paper under double-blind review



022 Figure 1: The landscape examples of ReactID for personalized video generation. For each case, ReactID
023 automatically plans a distinct action timeline for each reference subject, generating a final video where each
024 identity performs actions according to their synchronized schedule.

025 ABSTRACT

028 Personalized video generation faces a fundamental trade-off between identity con-
029 sistency and action realism: overly rigid identity preservation often leads to un-
030 natural motion, while emphasis on action dynamics can compromise subject fi-
031 delity. This tension stems from three interrelated challenges: imprecise subject-
032 video alignment, unstable training due to varying sample difficulties, and inad-
033 equate modeling of fine-grained actions. To address this, we propose ReactID,
034 a comprehensive framework that harmonizes identity accuracy and motion nat-
035 uralness through coordinated advances in data, training, and action modeling.
036 First, we construct ReactID-Data, a large-scale dataset annotated with a high-
037 precision pipeline combining vision-based entity label extraction, MLLM-based
038 subject detection, and post-verification to ensure reliable subject-video correspon-
039 dence. Second, we analyze learning difficulty along dimensions such as subject
040 size, appearance similarity, and sampling strategy, and devise a progressive train-
041 ing curriculum that evolves from easy to hard samples, ensuring stable conver-
042 gence while avoiding identity overfitting and copy-paste artifacts. Third, Reac-
043 tID introduces a novel timeline-based conditioning mechanism that supplements
044 monolithic text prompts with structured multi-action sequences. Each sub-action
045 is annotated with precise timestamps and descriptions, and integrated into the dif-
046 fusion model via two novel components: subject-aware cross-attention module to
047 bind sub-action to the specific subject of interest and temporally-adaptive RoPE
048 to embed the rescaled temporal coordinates invariant to action duration. Experi-
049 ments show that ReactID achieves state-of-the-art performance in both identity
050 preservation and action realism, effectively balancing the two objectives.

051 1 INTRODUCTION

052 The generation of high-fidelity video content has emerged as a pivotal task in computer vision and
053 graphics, with profound applications in content creation, virtual reality, and personalized media. A



Figure 2: An illustration of three key components in ReactID to improve personalized video generation from the perspectives of data construction, training paradigm and timeline formulation.

particularly challenging and impactful subset of this field is Personalized Video Generation, which aims to create video sequences of a specific subject (e.g., a person or object) performing a desired action while maintaining the identity of subject across frames. The core challenge in this task lies in achieving an optimal balance between two competing objectives: *preserving the identity of subject with high fidelity* and *ensuring the realism and naturalness of the generated actions*.

Current state-of-the-art approaches (Chen et al., 2025; Huang et al., 2025; Fei et al., 2025; Liu et al., 2025; Hu et al., 2025a; Jiang et al., 2025), typically built upon diffusion-based architectures, attempt to approach personalized video generation by incorporating reference identity information through cross-attention mechanisms or adapter modules. Despite the promising results, these methods consistently fall short of achieving the ideal balance between identity consistency and action realism. We speculate that this limitation stems from three fundamental bottlenecks in the generation pipeline, each contributing to the imbalance in different ways:

- (1) **Inaccurate identity preservation** resulting from noisy subject-video correspondences directly undermines the identity aspect of the balance. Conventional annotation pipelines often produce incomplete subjects, misaligned bounding boxes, and erroneous identity associations. When models learn from such imperfect supervision, they develop unreliable identity representations, leading to either identity drift or visual artifacts in generated videos.
- (2) **Unstable convergence patterns** caused by varying learning difficulties across samples disrupt the training process itself. Easy samples (with large, clear, and temporally consistent entities) encourage the model to adopt a “copy-paste” strategy, preserving identity at the expense of natural motion. Conversely, hard samples (with small scale, or appearance variations), though slowing convergence and complicating identity alignment, serve a critical function: they compel the model to maintain and leverage its pre-trained generative priors, thereby enhancing realistic action synthesis and mitigating catastrophic forgetting of motion dynamics.
- (3) **Compromised action naturalness** often results from coarse-grained action modeling that fail to capture temporal dynamics. Without precise temporal guidance, models tend to prioritize identity features—which are more explicitly supervised—over motion patterns, resulting in stiff, unnatural movements that diminish the overall realism of generated videos.

In this paper, we propose **ReactID**, a comprehensive framework designed to synchronize realistic action generation with faithful identity preservation through synergistic improvements across data curation, training strategy, and action modeling, as illustrated in Figure 2. Specifically, we first introduce ReactID-Data, a large-scale dataset with unprecedented annotation quality, enabled by a novel automated pipeline that leverages vision-based entity word extraction, Multi-modality Large Language Models (MLLM) based detection and additional post-verification to ensure reliable subject-video correspondences. Then, we develop a difficulty-aware progressive learning strategy that explicitly manages sample difficulty based on subject size, appearance similarity, and sampling strategy. Our curriculum learning approach ensures stable convergence while preventing both overfitting to easy samples and underfitting on challenging ones. To enable the modeling of complex, multi-action sequences, ReactID exploits a structured timeline-based conditioning mechanism complement to the conventional use of a single, monolithic text prompt for video generation. This timeline is composed of multiple fine-grained sub-actions, each annotated with precise start and end times alongside a detailed textual description of the specific motion. To effectively inject this rich spatio-temporal information into a diffusion-based generator, we introduce two key novel components: a subject-aware cross-attention module and a temporally-adaptive RoPE mechanism. The former embeds the rescaled temporal coordinates of the sub-actions, enhancing the compatibility and robustness to actions of varying lengths. The latter explicitly binds the descriptive sub-action

108 cues to the specific subject of interest within the scene, ensuring that the generated motions are accurately associated with the correct subject. This synergistic integration enables ReactID to achieve 109 unprecedented control over personalized video generation, seamlessly synchronizing realistic 110 actions with subject identity.

112 The main contributions of this work are summarized as follows. We propose ReactID, an innovative 113 framework that effectively harmonizes identity preservation and action realism in personalized video 114 generation. To support this framework, we introduce a large-scale, high-precision dataset (ReactID- 115 Data), a progressive training strategy that transitions from easy to difficult samples, and a novel 116 modeling architecture capable of representing complex multi-action sequences. Through extensive 117 experiments, ReactID demonstrates state-of-the-art performance in both identity consistency and 118 motion naturalness. Moreover, we believe the release of ReactID-Data with its temporally-precise 119 multi-action annotations will significantly facilitate future research in personalized video generation.

120

121

122

123 2 RELATED WORK

124

125

126 **Video Diffusion Models.** Recently, text-to-video (T2V) generation has witnessed remarkable 127 progress, largely driven by advances in diffusion models. Early attempts (Blattmann et al., 2023; 128 Guo et al., 2024; Zhang et al., 2024; 2025b) built on UNet (Ronneberger et al., 2015) architecture are 129 restricted to synthesize short clips with limited spatial and temporal resolution. Facing the unpre- 130 ceented capability demonstrated by Sora (Brooks et al., 2024) in generating high-quality, minute-long 131 videos, transformer-based diffusion models (Peebles & Xie, 2023) are increasingly introduced as 132 the mainstream, replacing UNet backbones and enabling scalable video generative models. Among 133 these, MMDiT (Esser et al., 2024), a dual-stream DiT architecture introduced by Stable Diffusion 134 3, is subsequently adopted in open-source video diffusion projects such as CogVideoX (Yang et al., 135 2025) and HunyuanVideo (Kong et al., 2024). More recently, Wan et al. (2025) leverage a attention- 136 based structure in video DiT, and achieve remarkable performance in realistic video generation.

137

138 **Personalized Video Generation.** The field of personalized video generation has witnessed a rapid 139 evolution from early UNet-based approaches (Chefer et al., 2024; He et al., 2024b; Ma et al., 2024; 140 Wu et al., 2024; Wang et al., 2024b; Zhou et al., 2024; Chen et al., 2024; Wu et al., 2025) to ad- 141 vanced Diffusion Transformer (DiT) architectures (Yuan et al., 2025b; Zhang et al., 2025a; Wei 142 et al., 2025a). Initial efforts on UNet were often confined to simple single-subject scenarios (He 143 et al., 2024b; Ma et al., 2024; He et al., 2024b; Jiang et al., 2024; Wei et al., 2024b), struggling 144 with limited motion and the need for extensive test-time tuning (Wei et al., 2024a; Wu et al., 145 2024). DreamVideo (Wei et al., 2024a) first decouples the learning for subject and motion. Cus- 146 tomCrafter (Wu et al., 2025) finetunes self-attention layers to enable subject customization without 147 disrupting the inherent motion modeling. With the paradigm shift to DiT frameworks, recent works 148 have substantially advanced visual fidelity and tuning-free capabilities. Owing to the scalable nature 149 of DiT, the scope of personalization has been broadened to encompass complex multi-subject and 150 open-domain settings (Huang et al., 2025; Chen et al., 2025; Liu et al., 2025; Jiang et al., 2025; 151 Fei et al., 2025; Hu et al., 2025a; Deng et al., 2025; Hu et al., 2025b). Moreover, customization 152 learning are not limited to visual appearance and identity, but also extended to relations and interac- 153 tions. Pioneering this direction, ReVersion (Huang et al., 2024) proposes a diffusion-based relation 154 inversion framework to capture specific relation from images, which is further employed for im- 155 age generation. DreamRelation (Wei et al., 2025b) further extends such type of relation modeling 156 into video synthesis. Despite these advancements, a key challenge persists: the inherent trade-off 157 between subject identity preservation and accurate motion generation often results in “copy-paste” 158 artifacts and unnatural motion. Compounding this issue is the scarcity of high-quality training data, 159 which remains a primary bottleneck. This underscores the urgent need for datasets with high action 160 prompt precision, video temporal consistency, and reference image diversity.

161 **In summary**, our work mainly focuses on preserving subject identity with high fidelity and ensuring 162 natural actions in personalized video generation. The proposal of ReactID contributes by studying 163 not only how to conduct progressive subject-to-video learning for accurate identity preservation 164 while alleviating “copy-paste” artifacts, but also how to integrate the timeline information into video 165 diffusion to achieve precise action realism.

162 3 METHOD
163164 3.1 REACTID-DATA: A DATASET FOR PERSONALIZED VIDEO GENERATION
165166 **Data Preparation.** We initialize a pool of 20 million videos from publicly available video collections such as HD-VG-130M (Wang et al., 2025) and OpenHumanVid (Li et al., 2025). Then we employ a pipeline to process raw videos, which involves key stages such as scene detection, video transcoding, text removal, quality assessment and filtering, and subject-centric captioning. The implementation details for this workflow are elaborated in the supplementary materials.
167
168
169
170171 **Entity Extraction.** A typical method to identify entities from video captions is to extract nouns via a Named Entity Recognition (NER) model (e.g., SpaCy (Honnibal & Montani, 2017)) with a pre-defined taxonomy. However, the limited taxonomy results in coarse-grained entities that cannot distinguish between different instances, especially for living subjects. For instance, two distinct individuals might both be labeled simply as “a person.” To mitigate this issue, we process living and non-living subjects differently. We first construct a 1200-term taxonomy by combining nouns from captions with labels from image datasets (e.g., Deng et al. (2009), Caesar et al. (2018), and Shao et al. (2019)), and then divide the terms into living and non-living categories. For each video-caption pair, an NER model guided by our taxonomy is employed to extract all entities from the caption. Entities identified as non-living subjects are directly retained as the final result, whereas those corresponding to living subjects undergo further processing. For these cases, a vision-language model analyzes the video content to generate a fine-grained, descriptive entity label for each living subject. As a result, we obtain specific entity labels for living subjects like “the person in red” and “the person sitting on the bench”, rather than generic ones such as “a person” and “another person”, enabling more precise entity referencing, which is crucial for the following processing.
172
173
174
175
176
177
178
179
180
181
182
183
184185 **Subject Detection and Segmentation.** Next, extracted entities are grounded to specific spatio-temporal regions within the video via subject detection and segmentation, thus forming comprehensive entity annotations. The primary challenge in this process lies in distinguishing between visually/semantically similar subjects and ensuring their correct association with the corresponding entities. To achieve this, an MLLM-based detector, Florence-2 (Xiao et al., 2024), is employed to locate the bounding boxes of the given entity labels, which are further verified by examining the cross-modal distance in the SigLIP (Zhai et al., 2023) feature space. Conditioning on the bounding boxes, we obtain the segmentation masks via the SAM (Ravi et al., 2024) model for each entity. Moreover, to better support face-centric identity-preserving generation tasks, we additionally extract face bounding boxes and masks for “human” entities utilizing the InsightFace Toolbox (Deng et al., 2019) and the SAM model, respectively.
186
187
188
189
190
191
192
193
194
195196 3.2 DIFFICULTY-AWARE CURRICULUM LEARNING
197198 A training sample consists of one or more reference images I_{ref} cropped from a subject’s bounding box, a video clip in which the subject appears V_{gt} , and a video caption $text$. Easy samples, where the subject in the video is large and highly similar to the reference, can encourage a “copy-paste” shortcut that harms generalization. In contrast, harder samples with small or varied subjects in videos force the model to learn the desired skill of fusing identity in I_{ref} with action and context provided in $text$, but they also present a convergence challenge. To balance the easy and hard samples and effectively leverage our ReactID-Data, we introduce an easy-to-hard curriculum learning strategy that ensures stable convergence while avoiding identity overfitting and “copy-paste” artifacts. Technically, we formalize this difficulty-aware learning by quantifying sample difficulty using three cues: subject size, appearance similarity, and sampling strategy.
199
200
201
202
203
204
205
206
207208 **Subject size** refers to the spatial proportion of the subject within the video frames. We define the 209 difficulty score \mathcal{D}_{sub} for each sample. Let the video V_{gt} consist of N frames, each with a resolution 210 of $H \times W$. For the n -th frame, a binary segmentation mask M_n is used, where $M_n(i, j) = 1$ 211 indicates that the pixel belongs to the subject in the reference image. The difficulty is calculated as:
212

213
$$\mathcal{D}_{sub} = 1 - (NHW)^{-1} \sum_{n=1}^N \sum_{i=1}^H \sum_{j=1}^W \mathbf{1}_{\{M_n(i, j) = 1\}} , \quad (1)$$

214

215 where $\mathbf{1}_{\{\cdot\}}$ is the indicator function. This formulation ensures that a smaller subject yields a higher difficulty score \mathcal{D}_{sub} , which approaches 1.

216 **Appearance similarity** quantifies the identity alignment between the reference image I_{ref} and the
 217 subject’s appearance in the video. We measure this by first detecting all N subject regions $\{P_i\}_1^N$ in
 218 the video and then calculating the average cosine similarity between the feature embeddings of I_{ref}
 219 and each P_i . The difficulty score \mathcal{D}_{app} is defined as:
 220

$$221 \quad \mathcal{D}_{app} = 1 - N^{-1} \sum_{i=1}^N [\mathcal{F}(I_{ref}) \cdot \mathcal{F}(P_i)] / [\|\mathcal{F}(I_{ref})\| \cdot \|\mathcal{F}(P_i)\|] , \quad (2)$$

223 where $\mathcal{F}(\cdot)$ is DINOv2 (Oquab et al., 2023) for general subjects and ArcFace (Deng et al., 2019) for
 224 faces. This formulation ensures that lower similarity results in a higher score.

225 **Sampling strategy** evaluates difficulty based on whether the reference image and video originate
 226 from the same clip. We define two strategies: *intra-clip sampling* (easy, $\mathcal{D}_{sam} = 0$), and *inter-clip*
 227 *sampling* (hard, $\mathcal{D}_{sam} = 1$). In intra-clip sampling, the reference I_{ref} is taken directly from the
 228 video V_{gt} , ensuring high visual consistency (lighting, background). Conversely, inter-clip sampling
 229 pairs the video with a visually similar reference from a different clip, forcing the model to handle
 230 greater variation and thus posing a more challenging learning task.

231 Finally, to obtain a single, comprehensive difficulty metric for each training sample, we compute a
 232 weighted sum of the scores from the three cues: $\mathcal{D}_{overall} = \lambda_{sub}\mathcal{D}_{sub} + \lambda_{app}\mathcal{D}_{app} + \lambda_{sam}\mathcal{D}_{sam}$,
 233 where the λ_{sub} , λ_{app} , and λ_{sam} are trade-off parameters that are determined empirically. During
 234 model training, we implement our curriculum by imposing a difficulty threshold τ and only samples
 235 where $\mathcal{D}_{overall} \leq \tau$ are used for training. As the training progresses, the threshold τ is increased in a
 236 multi-step schedule, progressively introducing more challenging examples for training. We pre-sort
 237 the training data according to the difficulty score $\mathcal{D}_{overall}$ and derive the difficulty threshold τ from
 238 the statistical quartiles of the score distribution. Following the ratio of 4:2:1:1, we partition the total
 239 training steps into four phases. At the transition of each phase, τ is stepped up to the next quartile.
 240 After each update point, the threshold remains fixed until the next scheduled change.

241 3.3 TEMPORAL-AWARE ACTION MODELING

243 3.3.1 TIMELINE ANNOTATION CONSTRUCTION

244 Modern text-to-video and subject-to-video datasets normally construct the training data as the pair
 245 of text-video or the triplet of text-video-reference, and the granular timeline information of actions
 246 is scarcely provided. The lack of temporal annotation could limit the model capacity to characterize
 247 sophisticated time-related action generation. In the scenario of personalized video generation,
 248 exploiting additional timeline information in training can further precisely regulate the fine-grained
 249 sub-action generation, facilitating the synthesis of more natural motion dynamic. To obtain such
 250 time-aware information for training, we sample a subset with 1.2M subject-to-video pairs from the
 251 ReactID-Data, and further construct the detailed timeline annotations for each video.

252 Specifically, we devise an ensemble approach that combines the vision language model (VLM), i.e.,
 253 Qwen2.5-VL-72B (Bai et al., 2025), with two visual temporal grounding models UniMD (Zeng
 254 et al., 2024) and TFVTG (Zheng et al., 2024) for timeline annotation construction. The VLM is
 255 responsible for initial temporal localization of events, and the two grounding models provide additional
 256 two sets of timestamp based on the initial captions generated by Qwen. Finally, we exploit
 257 another VLM, i.e., InterVideo2 (Wang et al., 2024a) as a scoring model to select the best candidates
 258 from the three annotations. Please refer Appendix B.2 for more details about the timeline annotation.

259 3.3.2 TEMPORAL-AWARE SUBJECT INTEGRATION

261 The overview of our ReactID is illustrated in Figure 3. To handle the subject timeline integration in
 262 diffusion, we introduce a novel subject-synchronized module which consists of two specific designs,
 263 i.e, subject-aware cross-attention and temporally-adaptive RoPE, in DiT blocks.

264 **Subject-Aware Cross-Attention.** For the subject-synchronized module as depicted in Figure 3, we
 265 exploit an attention-based mask predictor to estimate the mask for each subject, and further employ
 266 the masks to associate subject-related video latents and timeline prompts in cross-attention. In detail,
 267 we first compute the cross-attention map between reference image tokens and video tokens. Then,
 268 we feed the attention map into MLP for mask prediction for each subject, which is supervised by the
 269 ground-truth subject mask using a focal loss. To enhance the accuracy of subject mask prediction,
 we average all results from last five DiT blocks to obtain final subject masks. Next, we implement a

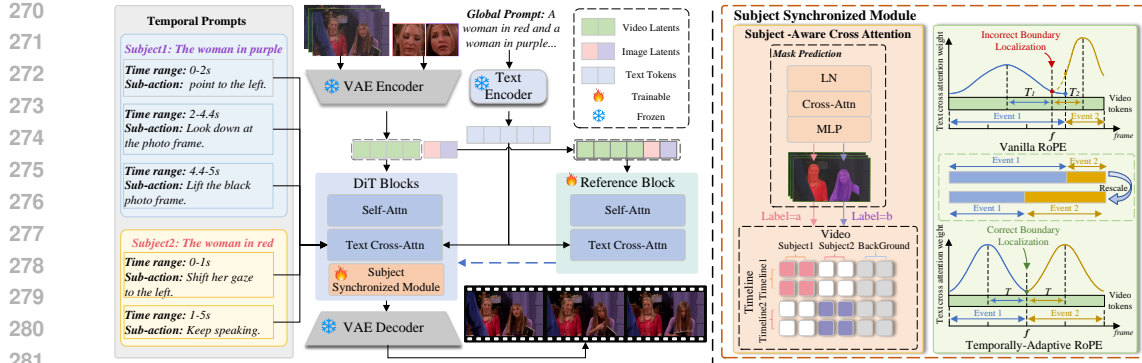


Figure 3: An overview of ReactID framework for personalized video generation.

label binding mechanism to establish explicit correspondence between subject-related video tokens and their sub-action timeline prompt in cross-attention. Specifically, we assigned a unique numerical label for subject-related video tokens located in the mask, and the corresponding timeline prompt receiving the same label. For instance, video tokens of “woman in red” receives label α , while video tokens of “woman in purple” is assigned label β . Video tokens falling outside all subject masks are classified as background and assigned a distinct label that differs from any subject label. Given the assigned labels, a label-dependent phase modulation is proposed to facilitate video tokens to primarily focus on their corresponding subject’s timeline while maintaining global interaction in cross-attention. The phase adjustments on both the query q_i (i.e., video tokens) and the key k_j (i.e., timeline prompt embeddings of each sub-action) are formulated as follows:

$$\tilde{q}_i = q_i e^{l_i \theta_0}, \quad \tilde{k}_j = k_j e^{l_j \theta_0}, \quad (3)$$

where l_i and l_j denote the assigned label value, and θ_0 is the base angle. Such phase adjustment ensures that the attention bias $\tilde{q}_i^\top \tilde{k}_j$ is maximized when label l_i and l_j match.

The subject-aware cross-attention guarantees that the video tokens with matched subject labels precisely attend to the timeline prompts at spatial level. The tokens with matching labels can be well-aligned, and those with mismatched labels are softly separated, ensuring the textual context embedded in the timeline annotations are correctly routed to the corresponding subject.

Temporally-Adaptive RoPE. In addition to spatial-level attention design to enhance subject and sub-action association, the precise timeline-aligned personalized video generation also necessitates the subject-action correlation modeling in temporal dimension. Vanilla temporal RoPE (Rotary Position Embedding) in attention exploits the absolute frame indices to construct the embedding, implicitly assuming that all sub-actions have the same duration. Nevertheless, the durations of sub-actions typically vary, and directly applying vanilla RoPE will lead to attention bias misalignment near the transition boundaries between two adjacent sub-actions. As demonstrated in Figure 3, the distance between the frame f and the midpoint of long sub-action is more than that between f and the midpoint of the subsequent short sub-action. Thus, f will perceive more attention bias to the midpoint of the short sub-action than the long sub-action when using vanilla RoPE. The allocation of attention bias is not reasonable since f belongs to the long sub-action, and this will lead to inaccurate temporal modeling and abrupt transitions. To alleviate this, we propose temporally-adaptive RoPE that rescales the temporal axis when constructing the temporal RoPE, which is invariant to the duration of various sub-action. Taking the frame index f that locates in n -th time interval $[f_n^{\text{start}}, f_n^{\text{end}}]$ as an example, the rescaled index f' is formulated as:

$$f' = (f - f_n^{\text{start}}) / (f_n^{\text{end}} - f_n^{\text{start}}) \cdot T + (n - 1) \cdot T, \quad \text{s.t. } f_n^{\text{start}} \leq f \leq f_n^{\text{end}}, \quad (4)$$

where T is a pre-defined constant that rescales each sub-action into a uniform temporal length.

Inference with Single Prompt. In addition to the personalized video generation using the structured timeline inputs, our ReactID can be readily extended for video generation given a single natural prompt. To enable this feature, we leverage LLMs to function as an automated temporal planner, which converts the single prompt into the timeline formats. The input prompt is first expanded into a detailed global description, and then decomposed into a sequence of distinct event captions, assigned with a plausible time interval for each sub-action. The obtained results are finally formed as structured timeline for ReactID to generate videos with realistic actions and identity preservation.

324 Table 1: Quantitative comparison of different approaches on the personalized video generation task across
 325 metrics: Aesthetics, Motion Smoothness, Motion Amplitude, Face Similarity, GmeScore, NexusScore, and
 326 NaturalScore. The best-performing result is highlighted in **bold**, and the second-best is underlined.

Method	Aes.↑	M. Smo.↑	M. Amp.↑	FaceSim↑	Gme.↑	Nexus.↑	Natural.↑	Total.↑
<i>OpenS2V-Eval: Single Domain</i>								
VACE-P1.3B	48.93%	<u>95.68%</u>	11.91%	18.04%	70.78%	36.24%	66.85%	49.20%
VACE-1.3B	49.41%	95.42%	<u>22.51%</u>	22.37%	<u>70.87%</u>	<u>38.34%</u>	<u>68.33%</u>	51.13%
Phantom-1.3B	49.00%	93.70%	16.38%	44.03%	69.54%	37.72%	66.76%	54.50%
ReactID	49.79%	96.25%	38.21%	<u>40.80%</u>	71.16%	39.85%	70.29%	56.04%
<i>OpenS2V-Eval: Human Domain</i>								
ID-Animator	42.03%	94.69%	33.54%	31.56%	52.91%	—	56.11%	49.75%
ConsisID	41.77%	79.83%	37.99%	43.19%	72.03%	—	55.83%	54.19%
EchoVideo	36.93%	77.96%	35.58%	<u>48.65%</u>	68.4%	—	62.22%	56.36%
FantasyID	45.60%	85.44%	23.41%	32.48%	72.68%	—	62.36%	54.33%
VACE-P1.3B	51.91%	95.80%	8.78%	19.98%	73.27%	—	65.83%	53.97%
VACE-1.3B	53.18%	<u>95.84%</u>	16.87%	22.29%	<u>73.61%</u>	—	65.28%	54.90%
Phantom-1.3B	50.80%	92.82%	14.99%	46.29%	72.17%	—	65.83%	60.00%
Concat-ID-Wan-AdaLN	43.13%	85.86%	17.19%	50.05%	71.90%	—	68.47%	59.85%
ReactID	<u>52.02%</u>	96.46%	40.79%	44.08%	73.96%	—	69.31%	62.17%
<i>ReactID-Eval-SEQ</i>								
VACE-P1.3B	46.59%	90.07%	15.81%	13.52%	69.83%	34.22%	60.68%	45.66%
VACE-1.3B	47.92%	<u>92.73%</u>	<u>23.65%</u>	19.48%	<u>70.02%</u>	35.18%	64.78%	48.58%
Phantom-1.3B	45.68%	92.16%	15.38%	<u>37.41%</u>	67.35%	38.69%	62.30%	51.40%
ReactID	49.11%	94.58%	39.46%	38.20%	71.23%	37.13%	68.69%	54.42%

4 EXPERIMENTS

4.1 EXPERIMENTAL SETTINGS

Datasets and Metrics. OpenS2V-Eval (Yuan et al., 2025a) is a fine-grained benchmark that contains 180 subject-text pairs focusing on the model’s ability to generate subject-consistent videos with natural subject appearance and identity fidelity. Moreover, to better assess the generation of complex, multi-action sequences, we introduce an evaluation set, ReactID-Eval-SEQ. It comprises 120 subject-text pairs, encompassing 40 human identities and 20 animals. The text prompt in each pair specifies sequential actions for the subject. Our evaluation methodology adheres to the OpenS2V-Nexus (Yuan et al., 2025a), employing seven scores to assess the generated videos: Aesthetics, Motion Smoothness, Motion Amplitude, Face Similarity, GmeScore, NexusScore, and NaturalScore. In line with the OpenS2V-Nexus protocol, all scores are normalized and then aggregated into a final TotalScore, with both processes following the procedures specified therein.

Implementation Details. We employ Wan2.1-T2V-1.3B (Wan et al., 2025) as our foundational model. Our ReactID model is trained for 10k steps with a global batch size of 32, utilizing the AdamW optimizer with a learning rate of 1×10^{-5} and 500 warmup steps. All training is conducted on 8 NVIDIA A100 GPUs, and consumes total 1,464 GPU hours. The averaged time of each optimization step is 65.8 seconds. Regarding the curriculum learning, we initialize the difficulty threshold τ at 0.53 and update it to 0.67, 1.44, and 1.84 at training steps 5k, 7.5k, and 8.75k, respectively. The ratio of inter-clip references within the total training samples is dynamically modulated by τ , adjusted to 0%, 0%, 11% and 33% at the corresponding update points. Since our proposal is insensitive to λ_{sub} , λ_{app} , and λ_{sam} , we empirically set them to 0.5, 1, 1, respectively, according to the relative importance of each dimension. For inference, we use 50 denoising steps and a classifier-free guidance (CFG) scale of 5.0. Generating a 5-second video requires about 316 seconds. An LLM (Achiam et al., 2023) is employed to convert prompts into a timeline format when necessary.

4.2 EVALUATION OF REACTID

Quantitative Results. In Table 1, we first present an analysis of our proposed ReactID in comparison with several open-source approaches on the OpenS2V-Eval across two scenarios: the Single Domain, which consists of test samples each containing a single subject drawn from various categories, and the Human Domain, which is composed solely of subjects from the ‘person’ category. All the mentioned baselines utilize foundational models with complexities comparable to ours, providing a fair basis for evaluation. In general, ReactID outperforms baselines across most metrics and achieves the highest overall scores in both domains. In the Single Domain, ReactID achieves superior performance across most metrics, including NexusScore, GmeScore, NaturalScore, and To-

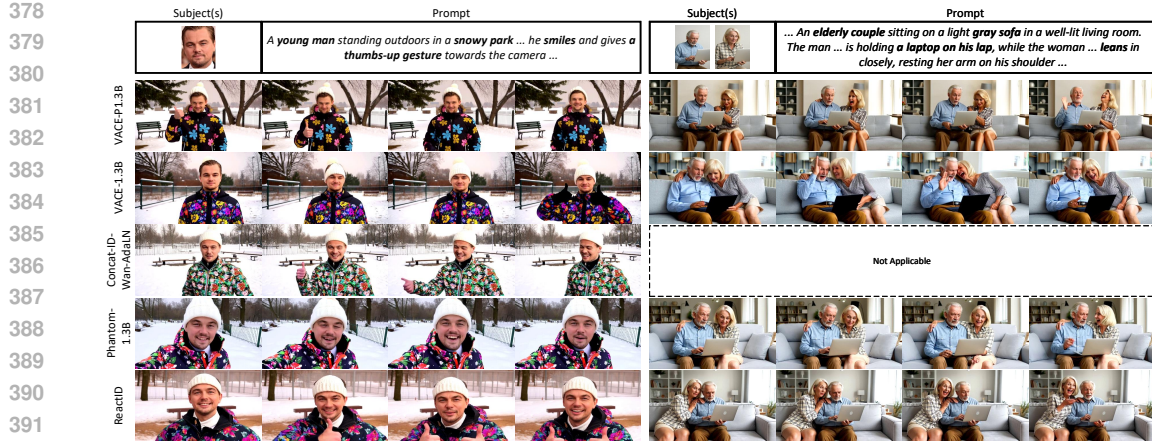


Figure 4: Qualitative comparisons of videos produced by different approaches on the OpenS2V-Eval dataset.



Figure 5: Comparisons of videos produced by different approaches on the ReactID-Eval-SEQ dataset.



Figure 6: Examples of video generation conditioned on multiple subjects and their respective timelines.

talScore. This highlights its capability to effectively harmonize subject consistency with action realism. However, it scores marginally lower than Phantom-1.3B on FaceSim. We attribute this deficit to ReactID generating more dynamic and natural movements (higher motion amplitude/smoothness), which may introduce motion blur, thereby reducing facial similarity to the reference image. In the Human Domain, ReactID achieves a TotalScore of 62.17%, surpassing the strongest of the seven baselines, Phantom-1.3B, by 2.17%. It also secures the top position in four out of the six available metrics (NexusScore is not applicable in this domain). Similar to the results in the Single Domain, ReactID achieves a competitive FaceSim score of 44.08% with a high Motion Amplitude of 40.79%. To further demonstrate ReactID’s advantages in generating videos with sequential actions, we conducted experiments on the ReactID-Eval-SEQ. We compared our model with three baseline approaches supporting both human and animal subjects. The results show that ReactID outperforms all baselines across most metrics. Notably, its TotalScore is 3.02% higher than the best competitor, which highlights ReactID’s capability for sequential action generation.

Qualitative Results. We proceed with a visual examination of the generation quality, comparing ReactID against four baselines (VACE-P1.3B, VACE-1.3B, Concat-ID-Wan-AdaLN, and Phantom-1.3B) on two input subject-text pairs. As illustrated in Figure 4, while all approaches successfully generate videos featuring the subjects from the reference images, our model produces the most plausible visual quality and naturalistic motions. Taking the left case as an example, ReactID adeptly generates a man in a snowy park giving a thumbs-up gesture. In contrast, the baseline VACE-P1.3B and VACE-1.3B struggles to preserve the subject’s key visual attributes from the reference image, leading to a degradation in subject consistency. While Phantom-1.3B effectively replicates the subject’s appearance, it fails to follow the text prompt and its video quality is compromised by “copy-paste” artifacts. These artifacts manifest as subjects appearing static or being unnaturally duplicated across frames, which results in visually implausible motion sequences.

432 Table 2: Comparisons between ReactID and four baselines with regard to human preference.
 433
 434
 435

Method	SC↑	AN↑	TVA↑	OVQ↑
ConsisID	1.97	1.66	2.13	1.84
ConcatID-WA	3.06	2.10	2.91	2.74
Phantom-1.3B	3.46	2.97	2.88	3.25
VACE-1.3B	3.23	3.20	3.08	3.37
ReactID	3.90	4.00	3.47	3.42

436 Table 3: Results on label binding in Subject-Aware Cross-Attention.
 437
 438

Method	FaceSim↑	Gme.↑	Natural.↑
<i>Label Strategy</i>			
Adaptive	48.42%	70.16%	66.24%
Uniform	49.11%	71.23%	68.69%
<i>Label Value Selection: (α, β)</i>			
(0, 1)	49.34%	70.08%	68.51%
(2, 20)	49.11%	71.23%	68.69%

439 Table 4: Ablation results on Temporally Adaptive RoPE in terms of strategy and rescale length.
 440
 441

Method	CLIP-T↑	TVA↑	TC↑
Attention Mask	0.241	2.62	2.25
Vanilla RoPE	0.242	2.67	2.35
TARoPE $T=8$	0.246	2.70	2.36
TARoPE $T=4$	0.247	2.69	2.35
TARoPE $T=2$	0.247	2.71	2.38

442 Table 5: Ablation study of the difficulty-aware curriculum learning in ReactID.
 443
 444

Method	Aes.↑	M. Smo.↑	M. Amp.↑	FaceSim↑	Gme.↑	Nexus.↑	Natural.↑	Total.↑
Full Data Training	48.19%	92.64%	37.22%	34.89%	69.16%	33.10%	65.13%	51.54%
Random Expansion	48.46%	92.56%	37.46%	34.74%	69.11%	33.24%	64.36%	51.39%
Curriculum w/o D_{sub}	48.43%	93.68%	35.27%	38.03%	70.68%	34.33%	68.01%	53.35%
Curriculum w/o D_{app}	48.96%	94.07%	38.84%	37.18%	71.16%	35.89%	68.14%	53.76%
Curriculum w/o D_{sam}	48.57%	93.26%	37.87%	35.76%	70.41%	35.06%	66.43%	52.68%
Full Curriculum	49.11%	94.58%	39.46%	38.20%	71.23%	37.13%	68.69%	54.42%

445 **Evaluation of ReactID-Data.** A comparative analysis of our ReactID-Data against OpenS2V-5M (Yuan et al., 2025a), which includes evaluations of data quality, human preference, and model training impact, is detailed in the supplementary materials.

446 **User Study.** We further conducted a user study to evaluate whether videos produced by ReactID better align with human preferences compared to those from four baseline methods: ConsisID, Concat-ID-Wan-AdaLN (ConcatID-WA), Phantom-1.3B, and VACE-1.3B. For this study, we randomly sampled 50 subject-text pairs from OpenS2v-Eval to serve as test cases. We recruited 25 evaluators (17 males, 8 females) with diverse educational backgrounds and ages. Each participant was asked to rate the generated videos on a 5-point Likert scale across four critical dimensions: (1) subject consistency (SC), (2) action naturalness (AN), (3) text-video alignment (TVA), and (4) overall visual quality (OVQ). To ensure a reliable assessment, the final score for each dimension was computed by averaging ratings across all participants and test cases. As presented in Table 2, ReactID demonstrates consistent superiority over all baselines across all four evaluated dimensions. This study thus validates the effectiveness of ReactID from a human perceptual standpoint.

461 4.3 ABLATION STUDY ON REACTID

462 In this section, we perform a series of ablation studies to delve into the design of ReactID for 463 personalized video generation. Note that all results here are evaluated on the ReactID-Eval-SEQ.

464 **Difficulty-aware Curriculum Learning.** We first delve into the effectiveness of our difficulty-aware 465 curriculum learning for personalized video generation, and report the performances in Table 5. When 466 progressively expanding the training set without using any difficulty guidance (i.e., **Random 467 Expansion**), the model achieves 51.39% TotalScore, which is lower than that of training with all 468 data (i.e., 51.54% achieved by **Full Data Training**). To ablate each component of difficulty-aware 469 curriculum learning, we conduct experiments by discarding any one of the three difficulty cues, and 470 the performances are superior to the baseline of no curriculum. By further exploiting all the three 471 cues in curriculum learning to avoid both overfitting to easy samples and underfitting on challenging 472 ones, ReactID with **Full Curriculum** learning shows the best 54.42% TotalScore.

473 **Subject-Aware Cross-Attention.** Then, we investigate different technical choices of label binding 474 strategies in subject-aware cross-attention of subject synchronized module. Table 3 details the 475 performances of two runs, i.e., adaptive labeling and our uniform labeling. **Adaptive labeling** assigns 476 varying label values based on predicted mask probabilities. The pixels with higher probability 477 receive larger values, while pixels with lower probability are assigned smaller ones. Instead, **Uniform 478 labeling** assigns a fixed label value to all pixels within each predicted subject mask. Counterintuitively, 479 the uniform labeling strategy outperforms the adaptive counterpart across all metrics. We 480 speculate that the results may be caused by the misalignment between the attended region derived 481 from mask probabilities and the region essential for personalized video generation. Compared to 482 potentially erroneous adaptive labeling, uniformly applying the same label to all tokens in the mask 483 can be more robust to attain better identity preservation. For the uniform labeling, we further explore 484 the influences of the labeling value selection. As indicated by the results, exploiting more distinct 485 label values (i.e., $\alpha = 2$ and $\beta = 20$) for different subjects empirically achieves better performances.

486
487 Table 6: Ablation study of de-
488 signs w.r.t. timeline.

Model	Data	TotalScore
Base	OpenS2V-5M	50.37%
Base	ReactID ⁻	52.14%
Base	ReactID	52.21%
ReactID	ReactID	54.42%

488 Table 7: Annotation quality
489 of timeline and mask.

Timeline Method	F1	Mask	
		Method	P. Rate
TFVTG	0.57	LISA	15%
InternVL	0.63	SAM	31%
Qwen	0.71	ReactID	54%
ReactID	0.78		

488 Table 8: User pref-
489 erence of timelines
490 from Expert/LLM.

Dims	LLM	Expert	PD
			GT
AO	46%	54%	
LC	48%	52%	
MN	53%	47%	

488 Table 9: Human Distin-
489 guishability of timelines
490 from Expert/LLM.

GT	LLM	Expert	PD
			GT
	52.8%	47.2%	
	47.8%	52.2%	

Temporally-Adaptive RoPE. We also explore different approaches of the RoPE design in temporal dimension for temporal alignment in ReactID. Two additional runs of attention masking and vanilla RoPE are conducted for comparison. **Attention masking** directly applies the temporal mask on video tokens to enforce the timeline prompt only attend to the corresponding frames, and there is no temporal RoPE implemented. **Vanilla RoPE** assigns original temporal RoPE to video tokens without temporal axis rescaling. In addition to utilize the metric of CLIP-T, we further leverage two measures from VideoScore (He et al., 2024a), i.e., Text-to-Video Alignment (TVA) and Temporal Consistency (TC) for temporal alignment evaluation. The performances of the three runs are summarized in Table 4. Compared to attention masking or vanilla RoPE that totally abandons RoPE or takes no account of event duration variances in temporal RoPE modeling, our temporally-adaptive RoPE dynamically adjusts the attention bias according to the sub-action duration in RoPE formulation, thereby achieving the best performances in temporal alignment. We also detail the performance comparisons by using different T . In practice, our ReactID yields the best results when T is 2.

Data Annotations. In Table 6, We quantify the impact of annotations in ReactID-Data by evaluating four model-data combinations on ReactID-Eval-SEQ. **Base** refers to the ReactID model without timeline-specific modules, while **ReactID⁻** denotes the ReactID-Data without timeline annotations. Base+ReactID⁻ outperforms Base+OpenS2V-5M, confirming that our data pipeline drives generation quality. Notably, naively incorporating timeline information as enhanced prompt (Base+ReactID-Data) yields negligible gains, suggesting the **Base** struggles to interpret complex temporal contexts from text alone. In contrast, our full model (ReactID+ReactID-Data) achieves the optimal performance, indicating that our timeline-related design is crucial to fully leverage the timeline information for accurate sub-action generation.

Subject Mask. To verify our carefully-minted subject mask generation, we conduct a user study on three methods: LISA, vanilla SAM and our proposal. For each mask, participants select the best one. As shown in Table 7, ours achieves the highest preference rate. Details are in Appendix E.1.

Timeline Annotation. We compare the quality of timeline annotation generated by ReactID and other methods via user study. As indicated by Table 7, the F1 score attained by ReactID is high than those of other methods, verifying our better quality. Please refer to Appendix E.2 for more details.

LLM-Planned Timelines. To evaluate the quality of our LLM-planned timelines, we conduct two user study, i.e., user preference (Table 8) across three dimensions (Action Order, Logical Coherence and Motion Naturlness) and distinguishability (Table 9) between human expert and LLM. The quality of videos generated on LLM-planned timelines are comparable to that of using expert-writing timelines, verifying the reliability of ours. More details are in Appendix E.3.

5 CONCLUSIONS

We have presented ReactID, a comprehensive framework devised to address the fundamental tension between identity preservation and action realism in personalized video generation. We identified and tackled the root causes of this problem, i.e., imprecise data alignment, unstable training, and inadequate action modeling, through a holistic approach. Our solution integrates three key components: a high-quality dataset (ReactID-Data) with reliable identity-video correspondence, a progressive training curriculum for stable learning, and a novel timeline-based conditioning mechanism for fine-grained action control. Extensive experimental results validate that ReactID achieves a new state-of-the-art performances, excelling in both maintaining subject identity and generating natural, complex motions. Beyond its immediate performance gains, we believe this work makes two pivotal contributions to the field. First, the release of the ReactID-Data dataset provides a critical foundation for future research, offering a benchmark for precise identity-action modeling. Second, our timeline-based paradigm demonstrates a scalable and intuitive path toward controllable, multi-action video synthesis, significantly broadening the potential applications of personalized generation.

540 **6 ETHICS STATEMENT**
541542 The primary of this paper is to introduce a personalized video diffusion model for reference subjects
543 to perform desired action while maintaining the identity across frames. In this work, we construct
544 our ReactID-Data from publicly available academic datasets. To ensure ethical compliance, we
545 strictly adhere to licensing policies and respect privacy rights. We only utilize publicly accessible
546 videos that are either explicitly licensed for research use or fall under fair-use considerations. No
547 copyrighted content is redistributed or modified in violation of licensing terms. We uphold the
548 highest ethical standards in the construction, use and dissemination of data.
549550 **7 REPRODUCIBILITY STATEMENT**
551552 The paper provides all necessary implementation details required to reproduce the main experimen-
553 tal results, including dataset processing procedure in Section 3.1 and Section B, model architectures,
554 training protocols in Section 3.2, hyperparameters and experimental settings in Section 4.1. Addi-
555 tionaly, we will release our constructed dataset for academic research, ensuring faithful reproduction
556 of our core results.
557558 **REFERENCES**
559560 Josh Achiam, Steven Adler, Sandhini Agarwal, Lama Ahmad, Ilge Akkaya, Florencia Leoni Ale-
561 man, Diogo Almeida, Janko Altenschmidt, Sam Altman, Shyamal Anadkat, et al. Gpt-4 technical
562 report. *arXiv preprint arXiv:2303.08774*, 2023.563 Shuai Bai, Keqin Chen, Xuejing Liu, Jialin Wang, Wenbin Ge, Sibo Song, Kai Dang, Peng Wang,
564 Shijie Wang, Jun Tang, et al. Qwen2.5-VL Technical Report. *arXiv preprint arXiv:2502.13923*,
565 2025.566 Andreas Blattmann, Tim Dockhorn, Sumith Kulal, Daniel Mendelevitch, Maciej Kilian, Dominik
567 Lorenz, Yam Levi, Zion English, Vikram Voleti, Adam Letts, et al. Stable video diffusion: Scaling
568 latent video diffusion models to large datasets. *arXiv preprint arXiv:2311.15127*, 2023.569 Tim Brooks, Bill Peebles, Connor Holmes, Will DePue, Yufei Guo, Li Jing, David Schnurr, Joe
570 Taylor, Troy Luhman, Eric Luhman, Clarence Ng, Ricky Wang, and Aditya Ramesh. Video
571 generation models as world simulators. Technical report, OpenAI, 2024.572 Holger Caesar, Jasper Uijlings, and Vittorio Ferrari. Coco-stuff: Thing and stuff classes in context.
573 In *CVPR*, 2018.574 Hila Chefer, Shiran Zada, Roni Paiss, Ariel Ephrat, Omer Tov, Michael Rubinstein, Lior Wolf, Tali
575 Dekel, Tomer Michaeli, and Inbar Mosseri. Still-moving: Customized video generation without
576 customized video data. *ACM Trans. Graph.*, 2024.577 Hong Chen, Xin Wang, Yipeng Zhang, Yuwei Zhou, Zeyang Zhang, Siao Tang, and Wenwu Zhu.
578 Disenstudio: Customized multi-subject text-to-video generation with disentangled spatial control.
579 In *ACM MM*, 2024.580 Tsai-Shien Chen, Aliaksandr Siarohin, Willi Menapace, Yuwei Fang, Kwot Sin Lee, Ivan Sko-
581 rokhodov, Kfir Aberman, Jun-Yan Zhu, Ming-Hsuan Yang, and Sergey Tulyakov. Multi-subject
582 open-set personalization in video generation. In *CVPR*, 2025.583 Jia Deng, Wei Dong, Richard Socher, Li-Jia Li, Kai Li, and Li Fei-Fei. Imagenet: A large-scale
584 hierarchical image database. In *CVPR*, 2009.585 Jiankang Deng, Jia Guo, Niannan Xue, and Stefanos Zafeiriou. Arcface: Additive angular margin
586 loss for deep face recognition. In *CVPR*, 2019.587 Yufan Deng, Xun Guo, Yuanyang Yin, Jacob Zhiyuan Fang, Yiding Yang, Yizhi Wang, Shenghai
588 Yuan, Angtian Wang, Bo Liu, Haibin Huang, et al. Magref: Masked guidance for any-reference
589 video generation. *arXiv preprint arXiv:2505.23742*, 2025.

594 Patrick Esser, Sumith Kulal, Andreas Blattmann, Rahim Entezari, Jonas Müller, Harry Saini, Yam
 595 Levi, Dominik Lorenz, Axel Sauer, Frederic Boesel, et al. Scaling rectified flow transformers for
 596 high-resolution image synthesis. In *ICML*, 2024.

597

598 Zhengcong Fei, Debang Li, Di Qiu, Jiahua Wang, Yikun Dou, Rui Wang, Jingtao Xu, Mingyuan
 599 Fan, Guibin Chen, Yang Li, et al. Skyreels-a2: Compose anything in video diffusion transformers.
 600 *arXiv preprint arXiv:2504.02436*, 2025.

601

602 Yuwei Guo, Ceyuan Yang, Anyi Rao, Zhengyang Liang, Yaohui Wang, Yu Qiao, Maneesh
 603 Agrawala, Dahua Lin, and Bo Dai. Animatediff: Animate your personalized text-to-image diffu-
 604 sion models without specific tuning. In *ICLR*, 2024.

605

606 Xuan He, Dongfu Jiang, Ge Zhang, Max Ku, Achint Soni, Sherman Siu, Haonan Chen, Abhranil
 607 Chandra, Ziyan Jiang, Aaran Arulraj, et al. VideoScore: Building Automatic Metrics to Simulate
 608 Fine-grained Human Feedback for Video Generation. *arXiv preprint arXiv:2406.15252*, 2024a.

609

610 Xuanhua He, Quande Liu, Shengju Qian, Xin Wang, Tao Hu, Ke Cao, Keyu Yan, Man Zhou, and
 611 Jie Zhang. Id-animator: Zero-shot identity-preserving human video generation. *arXiv preprint
 612 arXiv:2404.15275*, 2024b.

613

614 Matthew Honnibal and Ines Montani. spacy 2: Natural language understanding with bloom embed-
 615 dings, convolutional neural networks and incremental parsing. *To appear*, 2017.

616

617 Teng Hu, Zhentao Yu, Zhengguang Zhou, Sen Liang, Yuan Zhou, Qin Lin, and Qinglin Lu. Hun-
 618 yuancustom: A multimodal-driven architecture for customized video generation. *arXiv preprint
 619 arXiv:2505.04512*, 2025a.

620

621 Teng Hu, Zhentao Yu, Zhengguang Zhou, Jiangning Zhang, Yuan Zhou, Qinglin Lu, and Ran Yi.
 622 Polyvivid: Vivid multi-subject video generation with cross-modal interaction and enhancement.
 623 *arXiv preprint arXiv:2506.07848*, 2025b.

624

625 Yuzhou Huang, Ziyang Yuan, Quande Liu, Qiulin Wang, Xintao Wang, Ruimao Zhang, Pengfei
 626 Wan, Di Zhang, and Kun Gai. Conceptmaster: Multi-concept video customization on diffusion
 627 transformer models without test-time tuning. *arXiv preprint arXiv:2501.04698*, 2025.

628

629 Ziqi Huang, Tianxing Wu, Yuming Jiang, Kelvin CK Chan, and Ziwei Liu. Reversion: Diffusion-
 630 based relation inversion from images. In *SIGGRAPH Asia 2024 Conference Papers*, 2024.

631

632 Yuming Jiang, Tianxing Wu, Shuai Yang, Chenyang Si, Dahua Lin, Yu Qiao, Chen Change Loy, and
 633 Ziwei Liu. Videobooth: Diffusion-based video generation with image prompts. In *CVPR*, 2024.

634

635 Zeyinzi Jiang, Chaojie Mao, Ziyuan Huang, Ao Ma, Yiliang Lv, Yujun Shen, Deli Zhao, and Jingren
 636 Zhou. Res-tuning: A flexible and efficient tuning paradigm via unbinding tuner from backbone.
 637 In *NeurIPS*, 2023.

638

639 Zeyinzi Jiang, Zhen Han, Chaojie Mao, Jingfeng Zhang, Yulin Pan, and Yu Liu. Vace: All-in-one
 640 video creation and editing. *arXiv preprint arXiv:2503.07598*, 2025.

641

642 Weijie Kong, Qi Tian, Zijian Zhang, Rox Min, Zuozhuo Dai, Jin Zhou, Jiangfeng Xiong, Xin Li,
 643 Bo Wu, Jianwei Zhang, et al. Hunyuandvideo: A systematic framework for large video generative
 644 models. *arXiv preprint arXiv:2412.03603*, 2024.

645

646 Hui Li, Mingwang Xu, Yun Zhan, Shan Mu, Jiaye Li, Kaihui Cheng, Yuxuan Chen, Tan Chen,
 647 Mao Ye, Jingdong Wang, et al. Openhumanvid: A large-scale high-quality dataset for enhancing
 648 human-centric video generation. In *CVPR*, 2025.

649

650 Lijie Liu, Tianxiang Ma, Bingchuan Li, Zhuowei Chen, Jiawei Liu, Qian He, and Xinglong
 651 Wu. Phantom: Subject-consistent video generation via cross-modal alignment. *arXiv preprint
 652 arXiv:2502.11079*, 2025.

653

654 Shilong Liu, Zhaoyang Zeng, Tianhe Ren, Feng Li, Hao Zhang, Jie Yang, Chunyuan Li, Jianwei
 655 Yang, Hang Su, Jun Zhu, et al. Grounding DINO: Marrying Dino with Grounded Pre-Training
 656 for Open-Set Object Detection. In *ECCV*, 2024.

648 Ze Ma, Daquan Zhou, Xue-She Wang, Chun-Hsiao Yeh, Xiuyu Li, Huanrui Yang, Zhen Dong, Kurt
 649 Keutzer, and Jiashi Feng. Magic-me: Identity-specific video customized diffusion. In *ECCV*,
 650 2024.

651 Maxime Oquab, Timothée Dariset, Théo Moutakanni, Huy Vo, Marc Szafraniec, Vasil Khalidov,
 652 Pierre Fernandez, Daniel Haziza, Francisco Massa, Alaaeldin El-Nouby, et al. Dinov2: Learning
 653 robust visual features without supervision. *arXiv preprint arXiv:2304.07193*, 2023.

654 William Peebles and Saining Xie. Scalable diffusion models with transformers. In *ICCV*, 2023.

655 Nikhila Ravi, Valentin Gabeur, Yuan-Ting Hu, Ronghang Hu, Chaitanya Ryali, Tengyu Ma, Haitham
 656 Khedr, Roman Rädle, Chloe Rolland, Laura Gustafson, Eric Mintun, Junting Pan, Kalyan Va-
 657 sudev Alwala, Nicolas Carion, Chao-Yuan Wu, Ross Girshick, Piotr Dollár, and Christoph Fe-
 658 ichtenhofer. Sam 2: Segment anything in images and videos. *arXiv preprint arXiv:2408.00714*,
 659 2024.

660 Olaf Ronneberger, Philipp Fischer, and Thomas Brox. U-net: Convolutional networks for biomed-
 661 ical image segmentation. In *MICCAI*, 2015.

662 Shuai Shao, Zeming Li, Tianyuan Zhang, Chao Peng, Gang Yu, Xiangyu Zhang, Jing Li, and Jian
 663 Sun. Objects365: A large-scale, high-quality dataset for object detection. In *ICCV*, 2019.

664 PaddleOCR Team. Paddleocr. *PaddleOCR Lab*, 2024a. URL <https://github.com/PaddlePaddle/PaddleOCR>.

665 PySceneDetect Development Team. Pyscenedetect: An open-source video scene detection tool.
 666 <https://www.scenedetect.com/>, 2024b.

667 Team Wan, Ang Wang, Baole Ai, Bin Wen, Chaojie Mao, Chen-Wei Xie, Di Chen, Feiwu Yu,
 668 Haiming Zhao, Jianxiao Yang, et al. Wan: Open and advanced large-scale video generative
 669 models. *arXiv preprint arXiv:2503.20314*, 2025.

670 Wenjing Wang, Huan Yang, Zixi Tuo, Huigu He, Junchen Zhu, Jianlong Fu, and Jiaying Liu. Swap
 671 attention in spatiotemporal diffusions for text-to-video generation. In *ICCV*, 2025.

672 Yi Wang, Kunchang Li, Xinhao Li, Jiashuo Yu, Yinan He, Guo Chen, Baoqi Pei, Rongkun Zheng,
 673 Zun Wang, Yansong Shi, et al. Internvideo2: Scaling foundation models for multimodal video
 674 understanding. In *ECCV*, 2024a.

675 Zhao Wang, Aoxue Li, Lingting Zhu, Yong Guo, Qi Dou, and Zhenguo Li. Customvideo: Customiz-
 676 ing text-to-video generation with multiple subjects. *arXiv preprint arXiv:2401.09962*, 2024b.

677 Jiangchuan Wei, Shiyue Yan, Wenfeng Lin, Boyuan Liu, Renjie Chen, and Mingyu Guo. Echovideo:
 678 Identity-preserving human video generation by multimodal feature fusion. *arXiv preprint
 679 arXiv:2501.13452*, 2025a.

680 Yujie Wei, Shiwei Zhang, Zhiwu Qing, Hangjie Yuan, Zhiheng Liu, Yu Liu, Yingya Zhang, Jingren
 681 Zhou, and Hongming Shan. Dreamvideo: Composing your dream videos with customized subject
 682 and motion. In *CVPR*, 2024a.

683 Yujie Wei, Shiwei Zhang, Hangjie Yuan, Xiang Wang, Haonan Qiu, Rui Zhao, Yutong Feng, Feng
 684 Liu, Zhizhong Huang, Jiaxin Ye, et al. Dreamvideo-2: Zero-shot subject-driven video customiza-
 685 tion with precise motion control. *arXiv preprint arXiv:2410.13830*, 2024b.

686 Yujie Wei, Shiwei Zhang, Hangjie Yuan, Biao Gong, Longxiang Tang, Xiang Wang, Haonan Qiu,
 687 Hengjia Li, Shuai Tan, Yingya Zhang, and Hongming Shan. Dreamrelation: Relation-centric
 688 video customization. In *ICCV*, 2025b.

689 Jianzong Wu, Xiangtai Li, Yanhong Zeng, Jiangning Zhang, Qianyu Zhou, Yining Li, Yunhai Tong,
 690 and Kai Chen. Motionbooth: Motion-aware customized text-to-video generation. In *NeurIPS*,
 691 2024.

692 Tao Wu, Yong Zhang, Xintao Wang, Xianpan Zhou, Guangcong Zheng, Zhongang Qi, Ying Shan,
 693 and Xi Li. Customcrafter: Customized video generation with preserving motion and concept
 694 composition abilities. In *AAAI*, 2025.

702 Bin Xiao, Haiping Wu, Weijian Xu, Xiyang Dai, Houdong Hu, Yumao Lu, Michael Zeng, Ce Liu,
 703 and Lu Yuan. Florence-2: Advancing a unified representation for a variety of vision tasks. In
 704 *CVPR*, 2024.

705

706 Zhuoyi Yang, Jiayan Teng, Wendi Zheng, Ming Ding, Shiyu Huang, Jiazheng Xu, Yuanming Yang,
 707 Wenyi Hong, Xiaohan Zhang, Guanyu Feng, Da Yin, Yuxuan Zhang, Weihan Wang, Yean Cheng,
 708 Bin Xu, Xiaotao Gu, Yuxiao Dong, and Jie Tang. Cogvideox: Text-to-video diffusion models
 709 with an expert transformer. In *ICLR*, 2025.

710

711 Shanghai Yuan, Xianyi He, Yufan Deng, Yang Ye, Jinfa Huang, Bin Lin, Jiebo Luo, and Li Yuan.
 712 Opens2v-nexus: A detailed benchmark and million-scale dataset for subject-to-video generation.
 713 *arXiv preprint arXiv:2505.20292*, 2025a.

714

715 Shanghai Yuan, Jinfa Huang, Xianyi He, Yunyang Ge, Yujun Shi, Liuhan Chen, Jiebo Luo, and
 716 Li Yuan. Identity-preserving text-to-video generation by frequency decomposition. In *CVPR*,
 717 2025b.

718

719 Yingsen Zeng, Yujie Zhong, Chengjian Feng, and Lin Ma. Unimd: Towards unifying moment
 720 retrieval and temporal action detection. In *ECCV*, 2024.

721

722 Xiaohua Zhai, Basil Mustafa, Alexander Kolesnikov, and Lucas Beyer. Sigmoid loss for language
 723 image pre-training. In *CVPR*, 2023.

724

725 Yunpeng Zhang, Qiang Wang, Fan Jiang, Yaqi Fan, Mu Xu, and Yonggang Qi. Fantasyid: Face
 726 knowledge enhanced id-preserving video generation. *arXiv preprint arXiv:2502.13995*, 2025a.

727

728 Zhongwei Zhang, Fuchen Long, Yingwei Pan, Zhaofan Qiu, Ting Yao, Yang Cao, and Tao Mei.
 729 TRIP: Temporal Residual Learning with Image Noise Prior for Image-to-Video Diffusion Models.
 730 In *CVPR*, 2024.

731

732 Zhongwei Zhang, Fuchen Long, et al. MotionPro: A Precise Motion Controller for Image-to-Video
 733 Generation. In *CVPR*, 2025b.

734

735 Minghang Zheng, Xinhao Cai, Qingchao Chen, Yuxin Peng, and Yang Liu. Training-free video
 736 temporal grounding using large-scale pre-trained models. In *ECCV*, 2024.

737

738

739

740

741

742

743

744

745

746

747

748

749

750

751

752

753

754

755

756 **A APPENDIX: CLARIFICATION OF USING LLMs**
757758
759 In the period of paper writing, we only exploit the Large Language Model (LLM), i.e., GPT-4,
760 for word polishing to improve the presentation quality. No LLMs contributes to the core scientific
761 methods, technical contents, or any substantive research contributions.762
763 **B APPENDIX: DETAILS OF REACTID-DATA CONSTRUCTION**
764765 **B.1 VIDEO DATA PREPARATION**
766767
768 We first collect a pool of 20 million videos from publicly available video datasets such as HD-VG-
769 130M (Wang et al., 2025) and OpenHumanVid (Li et al., 2025). To detect the scene transition and
770 partition long videos into single shot video clips, we utilize the PySceneDetect (Team, 2024b) to
771 coarsely find the cut points according to color and brightness variations. Then, we detect the potential
772 semantical transition points in videos using the cosine similarity of DINOv2 (Oquab et al.,
773 2023) features between adjacent frames. Video clips longer than 5 seconds are saved to files using
774 H.264 codec. To remove the text overlays, subtitles, and watermarks from videos, we use Pad-
775 dleOCR (Team, 2024a) to find all text regions throughout the video, then crop it to the largest
776 possible text-free area. Next, we apply a suite of automatic video quality assessment methods to
777 evaluate each video clip across multiple facets, including aesthetic quality, technical quality, and
778 motion dynamics, and filter out the clips with low scores in any of these dimensions. To provide
779 rich, subject-centric textual captions which are crucial for personalized video generation, we em-
780 ploy an off-the-shelf vision-language model (Qwen2.5-VL (Bai et al., 2025)), which is prompted
781 to analyze each subject appearing in the video and describe their physical appearance, correspond-
782 ing actions, and background environment. According to the descriptions, video clips that possibly
783 contain an excessive number of subjects (e.g., a crowd of people or a line of cars) are filtered out,
784 ensuring that the remaining videos clear focus on a limited number of subjects.785 **Video Scene Cut.** To prepare a high-quality video clip pool, we employ a systematic two-stage
786 strategy to partition long videos into semantically coherent clips. The process begins with a coarse,
787 content-aware segmentation using PySceneDetect. Subsequently, we refine these initial segments
788 with DINOv2, inserting additional cuts at temporal locations where the cosine similarity between
789 adjacent frame features drops below a predefined threshold. Finally, we retain all clips with durations
790 above 5 seconds, which are well-suited for personalized video generation model training.791 **Video Quality Filtering.** We implement a multi-dimensional video quality scoring mechanism:792
793 (1) **Aesthetic Score:** We utilize an improved aesthetic predictor to evaluate the visual appearance
794 of each clip, only retaining those with high aesthetic scores.
795
796 (2) **Motion Score:** To distinguish deliberate subject motion from incidental camera movement, we
797 compute optical flow using RAFT model. The foreground and background flows are calcu-
798 lated separately, and the final score is based on the foreground flow, effectively isolating and
799 quantifying subject-specific motion.
800
801 (3) **Content Purity:** We employ PaddleOCR to detect and remove frames containing overlaid text
802 or watermarks. Frames with OCR confidence scores above 0.7 are flagged, and the clip is
803 cropped to retain only clean visual content.
804
805 (4) **Technical Quality:** We assess the technical quality using DOVER model for data filtering.806 **Video Captioning.** Effective captions for personalized video generation must be subject-centric, de-
807 tailing the reference subject’s appearance and motion while incorporating relevant contextual cues
808 from the background environment. To meet this requirement, we employ Qwen2.5-VL-7B to gen-
809 erate rich descriptions. Moreover, we filter out any captions containing plural entity nouns. This
810 operation not only maintains a clear focus on a limited number of subjects, but also facilitates con-
811 sistency between the used textual prompts during training and inference.

810
811 B.2 DATASET ANNOTATION812
813 We further construct the timeline annotation based on the collected video data. There are four main
814 steps in this data processing stage, i.e., entity label extraction, subject detection and segmentation,
face detection and segmentation, and timeline prompt captioning.815
816 **Entity Label Extraction.** To accurately identify distinct entities, we adopt a hybrid strategy that
817 leverages both textual and visual information for entity labeling, mitigating the risk of error propagation
818 from the video recaptioning. (1) For object label extraction, a text-based approach is exploited,
819 which first pre-defines a taxonomy of common objects, and then use a NER model, i.e., SpaCy (Hon-
820 nibal & Montani, 2017), to parse the captions and extract relevant entity labels in the taxonomy. (2)
821 To deal with human and living subjects, we shift to a vision-based method to accurately discriminate
822 entities with similar semantics. We leverage Qwen2.5-VL model to analyze the video content and
823 extract unique, descriptive entity labels. The potential inaccuracies caused by the generated captions
824 can be alleviated, providing a more robust foundation for subsequent subject and face detection.825
826 **Subject Detection and Segmentation.** Conventional CLIP-based detectors like Ground-
827 ingDINO (Liu et al., 2024) can fail to distinguish semantically similar concepts due to the limitation
828 in understanding. To overcome this, we leverage an MLLM-based detector, i.e., Florence-2 (Xiao
829 et al., 2024), for highly accurate subject detection. To further verify label-subject correspondence,
830 we perform a subsequent classification step using SigLIP (Zhai et al., 2023) as post-verification. Fi-
831 nally, we apply SAM2.1 (Ravi et al., 2024) to generate segmentation masks for the detected subjects.
832 These masks are further refined using morphological operations to improve boundary precision.833
834 **Face Detection and Segmentation.** To detect high-quality human faces, we first utilize Insightface
835 toolbox on video frames with 2 FPS sampling rate. Then, we apply Non-Maximum Suppression with
836 a 25% overlap threshold to filter duplicates and remove outlier bounding boxes. For each unique
837 person, the detected faces are ranked by confidence, and five representative frames are uniformly
838 sampled. Finally, SAM2.1 model is employed to generate precise segmentation masks for these
839 selected frames, which are subsequently refined using morphological operations as well.840
841 **Timeline Prompt Captioning.** We devise an ensemble approach that combines the vision lan-
842 guage model (VLM), i.e., Qwen2.5-VL-72B (Bai et al., 2025), with two visual temporal grounding
843 models UniMD (Zeng et al., 2024) and TFVTG (Zheng et al., 2024) to obtain both timestamps
844 and the descriptions of sub-actions. First, we instruct Qwen2.5-VL-72B to identify and caption
845 each sub-action in the video based on meaningful action changes and detect the timestamps of each
846 sub-action. Next, utilizing these captions of each sub-action as queries, we employ UniMD and
847 TFVTG to independently re-localize the temporal boundaries. This process yields three distinct sets
848 of candidate annotations per sub-action: one originating directly from the Qwen2.5-VL-72B and two
849 derived from specialized visual temporal grounding models. Finally, we employ InterVideo2 (Wang
850 et al., 2024a) as a scoring model. For each candidate, we utilize the video and text encoders of
851 InterVideo2 to extract visual and textual representations from the video segment and the sub-action
852 caption, respectively. We then calculate the cosine similarity between these embeddings to serve as
853 an alignment score. The candidate timeline annotation (comprising both the timestamp and caption)
854 with the highest alignment score is selected as the final detection for each sub-action.

855 C APPENDIX: STATISTICAL ANALYSIS ON REACTID-DATA

856
857 Figure 7 further demonstrates a statistical analysis on our proposed ReactID-Data. We measure
858 the video dataset from the perspectives of duration, resolution, word sequence length of prompt,
859 aesthetic score, and motion score. The word cloud of entity label is also depicted to show the major
860 components of the detected subjects. According to the statistics, the duration of more than 97%
861 videos is longer than 5 seconds, and all videos have a resolution of at least 720P, guaranteeing the
862 high video quality for model training. Meanwhile, around 94% videos having ≥ 50 words in each
863 text prompt indicate that ReactID-Data can provide precise and comprehensive textual descriptions
864 for videos to enhance video generation learning. The distribution of motion score is very uniform,
865 reflecting that the training data can cover both relative static and dynamic scenes. In the word cloud,
866 the entities such as human (e.g., woman and man), animals (e.g., horse) and common objects (e.g.,
867 sofa and mug) have been included. The reasonable data composition of ReactID-Data highlights the
868 merit for precise personalized video generation modeling.

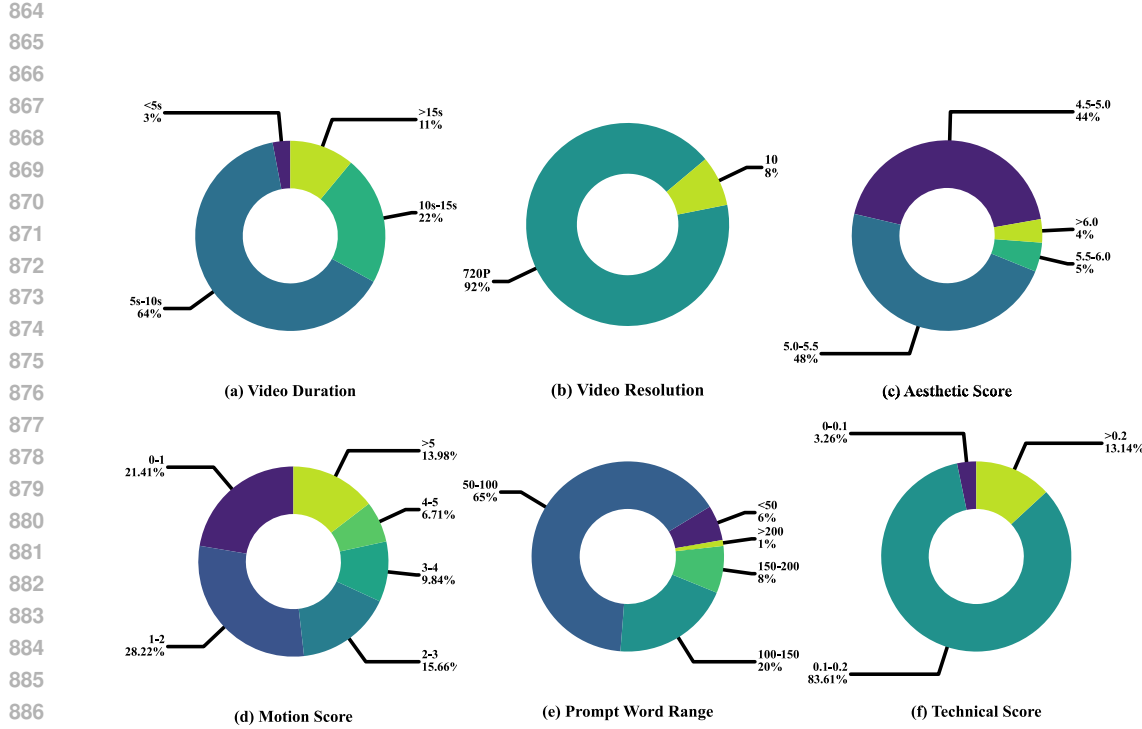


Figure 7: Statistical analysis on our ReactID-Data.



Figure 8: Examples of data items in the ReactID-Data.

D APPENDIX: OVERALL ARCHITECTURE OF REACTID

Given the subject-to-video pairs with timeline annotations, we proceed along the direction of typical personalized video generation DiT framework for subject condition injection, and further consider the timeline information learning. We choose the Wan2.1-1.3B (Wan et al., 2025) as the base architecture of our ReactID. To preserve the intrinsic capabilities of the original DiT blocks while enabling personalized video generation, we introduce a dedicated conditioning branch for reference image feature encoding. This conditioning branch consists of several reference blocks that are structurally identical to the base DiT blocks. We first apply the VAE on the reference images to obtain the image latents, which are treated as the condition and further fed into the condition branch. The extracted middle-level features from the image condition are then injected into the video diffusion model via Res-Tuning (Jiang et al., 2023) manner. To handle the subject timeline integration in diffusion, we introduce a novel subject-synchronized module which consists of two specific designs, i.e., subject-aware cross-attention and temporally-adaptive RoPE, in DiT blocks. The former ensures robust subject-action association in multi-subject scenarios by accurately binding each action to its corresponding subject. The latter precisely anchors each sub-action within the timeline to its designated timestamps, enhancing temporally alignment and semantically coherence.

918 E APPENDIX: MORE EVALUATION
919920 E.1 HUMAN EVALUATION ON SUBJECT MASK GENERATION
921

922 To obtain more accurate subject mask for our ReactID training, we improve the performance of
923 vanilla SAM (Ravi et al., 2024) segmentation pipeline by leveraging additional visual foundation
924 models and VLMs. First, we utilize SigLIP (Zhai et al., 2023) to filter out bounding boxes with low
925 image-text similarity to ensure that SAM receives correctly matched subject region for segmentation.
926 Then, we apply iterative morphological operations, including dilation and hole filling to improve
927 mask continuity. Finally, we employ Qwen2.5-VL-32B to score and verify the final mask quality.

928 To validate the effectiveness of our deliberate design, we conduct a human evaluation on 200 ran-
929 domly sampled cases. We recruit 20 participants from diverse backgrounds to perform a blind,
930 side-by-side comparison across three segmentation approaches: LISA (an MLLM-based segmen-
931 tation method), vanilla SAM and our method. For each sample, participants select the best mask. As
932 shown in the right part of Table 7, our pipeline achieves the highest preference rate, demonstrating
933 its effectiveness in reducing segmentation failures in challenging real-world scenarios.

934 E.2 HUMAN EVALUATION ON TIMELINE ANNOTATION
935

936 We conduct a user study to compare the quality of timeline annotation between our ReactID and
937 other VLMs or specialized models. Particularly, 20 participants are invited from diverse academic
938 and professional backgrounds. We randomly sample 200 timeline annotations from our dataset
939 for the human evaluation. Each participant is instructed to evaluate every annotation generated by
940 ReactID and other VLMs along two dimensions, event and timestamp accuracy. According to the
941 evaluation results, we classify the timeline annotations into three categories to compute the F1 score.

- 942 • False Negatives: When the annotation pipeline misses a salient event present in the video.
- 943 • False Positives: When the detected event does not exist in the video or the timestamp does not
944 match the event boundaries.
- 945 • True Positives: When both the caption and timestamp are correct.

946 As shown in the left part of Table 7, our ReactID achieves a superior F1 score of 0.78, supported
947 by a inter-annotator agreement of 0.86. The Qwen2.5-VL follows as the second-best annotator with
948 an F1 score of 0.71. The results reflect the robustness of our timeline generation pipeline, and the
949 precision of the timeline annotations to facilitate timeline-based generation model training.

950 E.3 HUMAN EVALUATION ON LLM-PLANNED TIMELINES
951

952 To evaluate the quality of our LLM-planned timelines for personalized video generation, we conduct
953 two types of human evaluations, i.e., user preference and distinguishability, between the timelines
954 generated by human expert and LLM. Specifically, we instruct 20 participants to evaluate 200 videos
955 generated on the human expert-annotated and our LLM-planned timelines across three dimensions:
956 Action Order (AO), Logical Coherence (LC), and Motion Naturalness (MN).

957 **User Preference.** The results in Table 8 demonstrate comparable human preference between the
958 generated videos using such two kinds of timelines. Notably, videos conditioned on LLM-planned
959 timelines even slightly outperform expert annotations in terms of Motion Naturalness, suggesting
960 superior fluidity in the generated content.

961 **User Distinguishability.** Table 9 further presents the confusion matrix of the human distinguisha-
962 bility test. As observed, evaluators could not reliably differentiate between the human-annotated or
963 our LLM-based sources. The evaluation indicate that our timeline annotation planned by LLM is
964 reliable and aligns closely with the human expert logic.

965 E.4 COMPARISON BETWEEN OPENS2V-5M AND REACTID-DATA
966

967 We conduct a comprehensive comparison between recent public OpenS2V-5M (Yuan et al., 2025a)
968 and our proposed ReactID-Data. First, we randomly select 2,000 samples from both OpenS2V-
969 5M and ReactID-Data, then employ CLIP to classify subject images against their corresponding

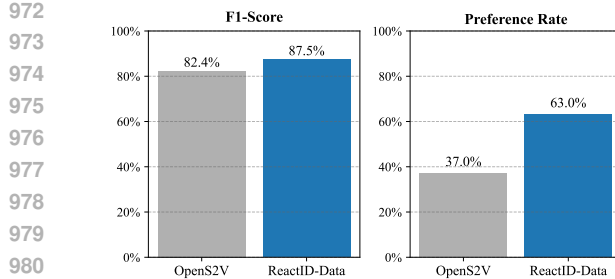


Figure 9: Classification and preference comparison between OpenS2V-5M and our ReactID-Data.

Table 10: Comparisons of ConsisID trained on different datasets. Models are evaluated on the ReactID-Eval-SEQ dataset.

Training Data	FaceSim \uparrow	Gme. \uparrow	Natural. \uparrow
OpenS2V-5M	45.12%	72.86%	59.51%
ReactID-Data	45.41%	73.20%	64.77%

Table 11: Quantitative comparison of different approaches on our ReactID-Eval-SEQ dataset. The best-performing result is highlighted in **bold**.

Method	Aes. \uparrow	M. Smo. \uparrow	M. Amp. \uparrow	FaceSim \uparrow	Gme. \uparrow	Nexus. \uparrow	Natural. \uparrow	Total. \uparrow
<i>Without Prompt Pre-processing</i>								
VACE-1.3B	47.92%	92.73%	23.65%	19.48%	70.02%	35.18%	64.78%	48.58%
Phantom-1.3B	45.68%	92.16%	15.38%	37.41%	67.35%	38.69%	62.30%	51.40%
<i>With LLM Enhanced Prompts</i>								
VACE-1.3B	48.20%	92.60%	23.45%	19.70%	70.00%	35.30%	64.90%	48.70%
Phantom-1.3B	45.80%	92.05%	15.25%	37.20%	67.50%	38.60%	62.40%	51.30%
<i>With LLM Planned Structured Timeline Prompts</i>								
VACE-1.3B	47.98%	92.78%	23.38%	19.25%	69.96%	35.05%	64.52%	48.25%
Phantom-1.3B	45.75%	92.10%	15.18%	37.05%	67.45%	38.50%	62.05%	50.95%
ReactID	49.11%	94.58%	39.46%	38.20%	71.23%	37.13%	68.69%	54.42%

entity labels. We compute F1-score to evaluate classification performance. As shown in left part of Figure 9, ours achieves significantly higher F1-scores, demonstrating the superiority of our data construction pipeline. When handling complex scenarios containing entities with high visual or semantic similarity, our pipeline can maintain precise entity labeling and accurate subject extraction. However, the commonly adopted text-based entity extraction approach (i.e., Grounded-SAM) in OpenS2V may suffer from omissions and misclassifications. To further validate the labeling quality of the two measurements, we conduct a human evaluation. Specifically, we randomly sample 2,000 valid instances from the HD-VG-130M dataset and process them using both the conventional data pipeline and our data pipeline. 25 participants are recruited to evaluate the quality of both datasets, specifically assessing whether subject extraction is accurate, complete, and consistent with the assigned labels. Each participant selects the better-processed result from the two alternatives. We report the average preference rate across all trials in the right part of Figure 9. There are 63% of participants that favor our data processing pipeline, compared to only 37% for the conventional approach. To further testify the quality of ReactID-Data, we train ConsisID from scratch under identical setting on 500K samples randomly selected from the OpenS2V-5M and ReactID-Data, respectively. As shown in Table 10, the model trained on ReactID-Data outperforms the model trained on equivalent data in OpenS2V-5M, confirming that our ReactID-Data facilitates superior model optimization in personalized video generation.

E.5 MODEL PERFORMANCES ON DIFFERENT PROMPT FORMATS

To analyze whether the existing models can be improved through enriched text prompts, we select two top-performing models, VACE-1.3B and Phantom-1.3B, and perform these two methods on the input prompts processed by two augmentation strategies: prompt enhancement and structured timeline prompts. The performances on OpenS2V are illustrated in Table 11. Prompt enhancement yields minimal performance gains across all baselines that generate videos without any prompt pre-processing. The results are expected since the majority of prompts in the OpenS2V already consist of detailed, comprehensive captions. Notably, for the models trained without timeline annotations, the structured timeline prompt also fails to deliver significant improvements and, in some cases, leads to performance degradation. This somewhat reveals a fundamental limitation: models not explicitly trained on timeline-structured data possess limited temporal reasoning capabilities, and cannot effectively leverage sequential action descriptions to enhance motion naturalness. Without designing



Figure 10: An additional example of ReactID. The model successfully generates a sequence of actions performed by the same person: basketball crossing-over, shooting, and singing.

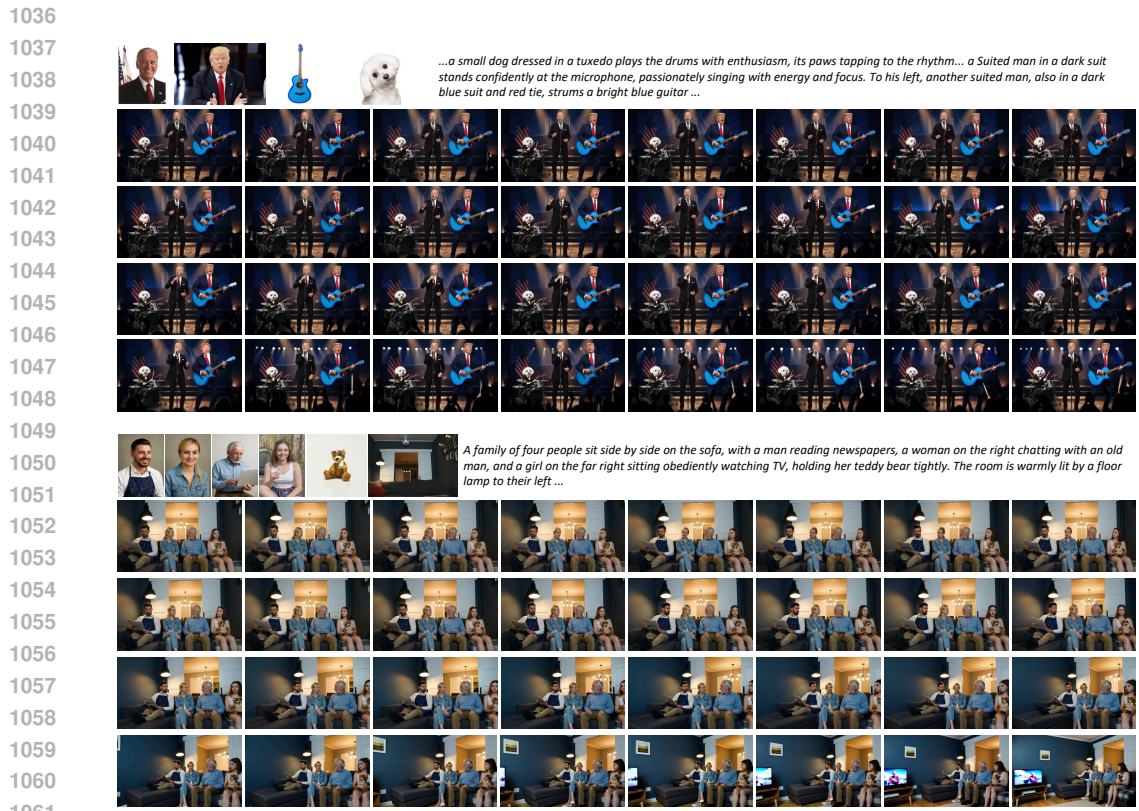
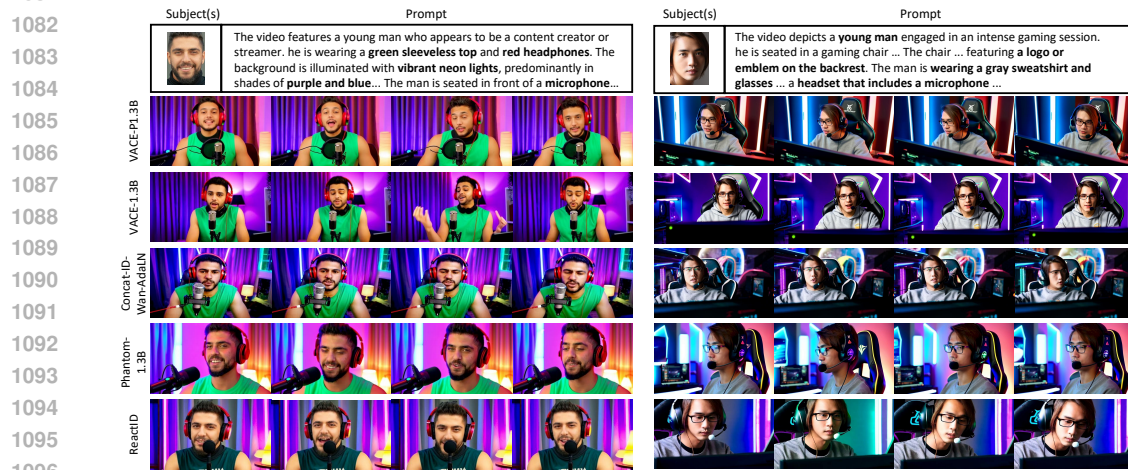


Figure 11: Visualization of two 30-second long videos generated by ReactID.

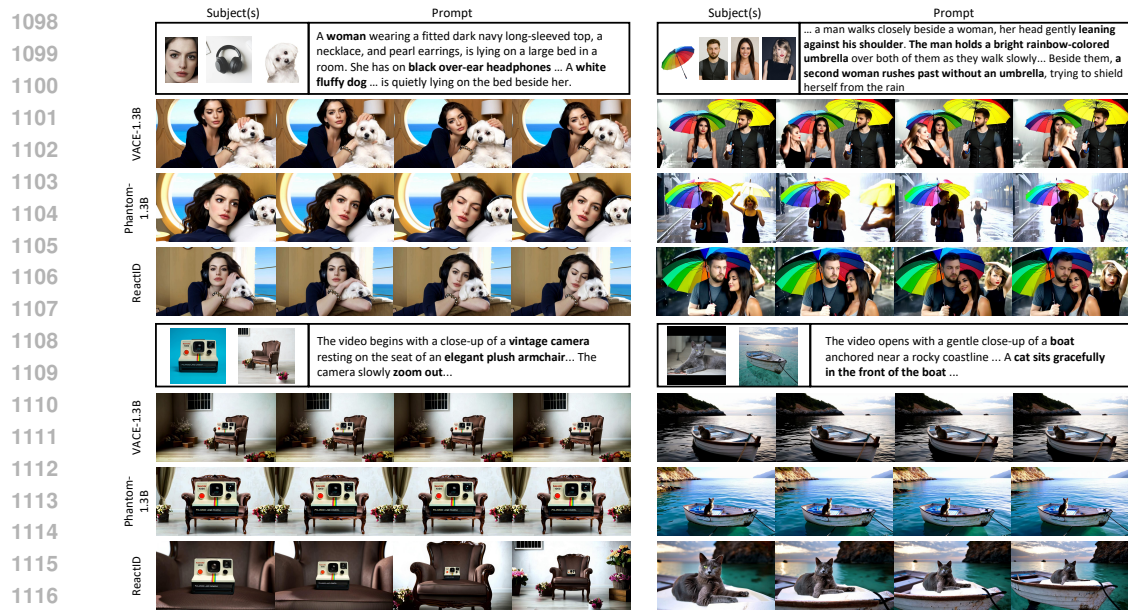
proper temporal modeling architectures, simply reformatting single text prompts into timeline structures may introduce confusion for action modeling in video generation. These findings underscore the importance of architectural design and training paradigms tailored for temporal action modeling, rather than solely relying on input formatting modifications.

E.6 LONG VIDEO GENERATION

Long video generation in personalized video generation generally suffers from identity drift, minimum or collapsed motion. Although ReactID was not explicitly optimized for long video generation, it can be effectively coupled with an auto-regressive generation strategy to generate longer videos while maintaining high identity consistency. Specifically, ReactID generates the video segment-by-segment (e.g., in 5-second clips), utilizing the preceding segments as the visual condition for the subsequent one. This iterative process allows us to customize videos extending well beyond the standard 5-second duration. As shown in Figure 11, we successfully generate long videos in multi-subject scenarios with four and six reference subjects while maintaining the identity of all subjects throughout the video, without significant temporal drift.

1080 E.7 ADDITIONAL VISUALIZATION
1081

1097 Figure 12: Additional comparative results of single-face customization across different methods.



1117 Figure 13: Additional comparative results of multi-subject customization across different methods.



1134 Figure 14: Additional results generated by ReactID.